Talanta 107 (2013) 225–232

Contents lists available at SciVerse ScienceDirect

Talanta

journal homepage: www.elsevier.com/locate/talanta

Comparison of reactant and analyte ions for ^{63}Nickel, corona discharge, and secondary electrospray ionization sources with ion mobility-mass spectrometry

C.L. Crawford, H.H. Hill *

Washington State University, Department of Chemistry, PO Box 644630, Pullman, WA 99164, USA

ARTICLE INFO

Article history:
Received 5 November 2012
Received in revised form
8 January 2013
Accepted 8 January 2013
Available online 17 January 2013

Keywords:
Ion mobility spectrometry
Mass spectrometry
Ionization
^{63}Nickel
Corona discharge
Secondary electrospray
Reactant ion chemistry

ABSTRACT

^{63}Nickel radioactive ionization (^{63}Ni) is the most common and widely used ion source for ion mobility spectrometry (IMS). Regulatory, financial, and operational concerns with this source have promoted recent development of non-radioactive sources, such as corona discharge ionization (CD), for stand-alone IMS systems. However, there has been no comparison of the negative ion species produced by all three sources in the literature. This study compares the negative reactant and analyte ions produced by three sources on an ion mobility-mass spectrometer: conventional ^{63}Ni, CD, and secondary electrospray ionization (SESI). Results showed that ^{63}Ni and SESI produced the same reactant ion species while CD produced only the nitrate monomer and dimer ions. The analyte ions produced by each ion source were the same except for the CD source which produced a different ion species for the explosive RDX than either the ^{63}Ni or SESI source. Accurate and reproducible reduced mobility (K_0) values, including several values reported here for the first time, were found for each explosive with each ion source. Overall, the SESI source most closely reproduced the reactant ion species and analyte ion species profiles for ^{63}Ni. This source may serve as a non-radioactive, robust, and flexible alternative for ^{63}Ni.

© 2013 Elsevier B.V. All rights reserved.

1. Introduction

The ^{63}Nickel (^{63}Ni) ion source is the most common source used in standalone, commercial ion mobility spectrometry (IMS) systems [1]. This ion source's prevalence is due in part to its long-term stability and reliable ion chemistry. The ^{63}Ni source produces negative reactant ions via the following mechanism:

$$\begin{aligned} &O_2 + e^- \rightarrow O_2^- \\ &H_2O + O_2^- \leftrightarrow O_2^- H_2O \\ &H_2O + O_2^- H_2O \leftrightarrow O_2^- (H_2O)_2 \end{aligned} \quad (1)$$

where the dominant reactant ion is a hydrated O_2^- ion [1]. This reactant ion is present in standalone systems using clean, dry air as both the sample and drift gas unless a more electronegative compound such as CH_2Cl_2 (commonly referred to as a dopant) is added to change the reactant ion chemistry [2–5]. The ^{63}Ni source also requires little or no maintenance and does not require an external power supply. However, there have been increasing financial, regulatory, and operational reasons to discontinue use of these sources and implement the use of non-radioactive ionization sources [6].

The second most common source in commercial, stand-alone systems is the corona discharge (CD) ionization source [7]. These sources are constructed in various configurations (e.g., point-to-plane geometry with a metal wire discharging to a metal surface) and operated in either a continuous or pulsed discharge mode [1]. The advantages of this source include greater ion current over the ^{63}Ni source, low cost assembly, and ease of operation [1]. The disadvantages of CD sources are the need for external high voltage supplies, long-term stability issues, and maintenance and/or replacement of the discharge component due to corrosion of the metal surface [1]. The pulsed operation may also induce time-dependent changes in the reactant ion chemistry and subsequent analyte ion chemistry [1,6,8]. This is due to the ionization mechanism which produces a cascading series of negative reactant ions through increasing concentrations of ozone and nitrogen dioxide neutrals: [9]

$$\begin{aligned} &O_2 + e^- + N_2 \rightarrow O_2^- + N_2 \\ &O_2^- + O_3 \rightarrow O_3^- + O_2 \\ &O_3^- + CO_2 \rightarrow CO_3^- + O_2 \\ &O_2^- + NO_2 \rightarrow NO_2^- + O_2 \\ &NO_2^- + O_3 \rightarrow NO_3^- + O_2 \end{aligned} \quad (2)$$

The reactant ion formation can be influenced by careful control of gas flow and concentration. When the corona discharge is pulsed on and off, this may prevent the buildup of ozone and

* Corresponding author. Tel.: +1 509 335 5648; fax: +1 509 335 8867.
E-mail address: hhhill@wsu.edu (H.H. Hill).

0039-9140/$ - see front matter © 2013 Elsevier B.V. All rights reserved.
http://dx.doi.org/10.1016/j.talanta.2013.01.009

nitrogen dioxide neutrals which, in turn, can lead to difficult operation [6,8,9]. A recent attempt has been made to address the long-term stability issues in CD sources by using an RF voltage applied on either side of a dielectric material. This new CD design has been termed distributed plasma ionization [10].

Secondary electrospray ionization (SESI) is a variant of electrospray ionization (ESI). Fundamental studies that first described SESI processes were performed by Fenn and co-workers. SESI was first developed for use as an ion source by Hill and used to analyze national security threats including explosives, chemical warfare agents, illicit drugs, and volatile organic chemicals (VOCs) in IMS, MS, and hybrid ion mobility mass spectrometers (IMMS) [11–18]. The SESI source consists of an electrospray apparatus with a fused silica or metal capillary for solvent introduction which connects to a high voltage source and is placed at the front of the IMS system's ion-molecule reaction region. Once neutral gas phase sample is quantitatively introduced into the ion-molecule reaction region of the IMS, one or more mechanisms may create ions. Separately, Fenn and Hill both suggested that interactions with the ESI droplets that contain the primary reactant ions and the neutral sample vapor produced ions with SESI. Fenn also suggested that charge exchange or chemi-ionization processes could create ions by SESI after desolvation of the ESI droplets [12,15,19,20].

Previous IMS research found that SESI achieved dynamic range gains over ^{63}Ni ionization and increased ionization efficiency and sensitivity over conventional atmospheric pressure chemical ionization (APCI) and electrospray ionization (ESI) [11,12,14]. This source can also introduce volatile and non-volatile dopants into the gas phase. Dopants are used to produce reactant ions in IMS; the radioactive source can only accommodate volatile dopants [2,13]. These reactant ions then provide a source of charge for ion-molecule charge transfer reactions. Disadvantages of this source include the need for an external high voltage supply, a solvent delivery system, and consumable costs for the solvent solutions (typically alcohol and DI water mixtures) [11].

When SESI was used to ionize vapor samples containing explosives, the SESI source provided lower detection limits for RDX over conventional ESI and ^{63}Ni ionization and greater response sensitivity for RDX, NG, and PETN using a non-volatile nitrate dopant instead of the traditional volatile chloride dopant [13]. Recently, SESI was used to achieve lower limits of detection for TNT and PETN on several atmospheric pressure ionization-mass spectrometers (API-MS) [16].

If gains are realized in detection sensitivity and specificity for explosives using an ionization source other than conventional ^{63}Ni, then a comparison of the proposed alternative sources' reactant and analyte ions must be performed. Table 1 summarizes the ion species and reduced mobility (K_0) values for explosives in the peer-reviewed literature for the CD and SESI ion sources (K_0 values are used to identify analytes in IMS); [1] a thorough review is available of the K_0 values produced by ^{63}Ni ionization sources for these explosives and others [21].

These summaries highlight problems with accurate ion species identification and K_0 value calculation. Specifically, there is a range of ion species for each explosive across the various ion sources. There is also a range of K_0 values for the same ion species found with the same source and across the ion sources. The determination of ion species produced by various ionization sources is important because the ion species determines the K_0 value for that analyte ion. If the analyte ion found with the ^{63}Ni source, used as a benchmark for portable and hand-held IMS systems, does not match the ion(s) produced for an explosive by another ion source, then the K_0 values will not match.

Correlation of K_0 values is especially critical when field-portable standalone IMS units are used for explosives and contraband

Table 1
Summary of reduced mobility values found in the literature for the CD, SESI, and ESI ion sources and for the explosives used in this study.

Compound	Species	K_0	Ion source	Mass ID.	Reference
TNT	$TNT-H^-$	1.55	CD	No	2003 Khaymian [26]
TNT	$TNT-H^-$	1.53	CD	No	2011 Roscioli [27]
TNT	$TNT-H^-$	1.58	CD	Yes	2009 Laakia [28]
TNT	$TNT-H^-$	N/A	SESI	Yes	2009 Fernandez [29]
TNT	$TNT-H^-$	1.59	ESI	No	2010 Hilton Wu [30]
TNT	TNT^-	1.55	CD	No	2002 Tabrizchi [31]
TNT	$TNT-NO^-$	1.97	CD	Yes	2009 Laakia [28]
TNT	$TNT+O^-$	1.53–1.55	CD	Yes	2009 Laakia [28]
NG	$NG+NO_3^-$	1.31	SESI	No	2004 Tam Hill [13]
NG	$NG+Cl^-$	1.40	SESI	No	2004 Tam Hill [13]
NG	$NG-H^-$	1.45	SESI	No	2004 Tam Hill [13]
RDX	$RDX+NO_3^-$	1.27	CD	No	2003 Khaymian [26]
RDX	$RDX+NO_3^-$	1.436	CD	Yes	2009 Ewing [9]
RDX	$RDX+NO_3^-$	1.46	CD	No	2011 Roscioli [27]
RDX	$RDX+NO_3^-$	1.35	SESI	No	2004 Tam Hill [13]
RDX	$RDX+NO_3^-$	1.42	ESI	No	2010 Hilton Wu [30]
RDX	$RDX+NO_2^-$	1.47	CD	No	2003 Khaymian [26]
RDX	$RDX+NO_2^-$	1.49	CD	Yes	2009 Ewing [9]
RDX	$RDX+NO_2^-$	1.40	SESI	No	2004 Tam Hill [13]
RDX	$RDX+NO_2^-$	1.48	ESI	No	2010 Hilton Wu [30]
PETN	$PETN+NO_3^-$	1.21	CD	No	2003 Khaymian [26]
PETN	$PETN+NO_3^-$	1.21	CD	No	2002 Tabrizchi [31]
PETN	$PETN+NO_3^-$	1.10	CD	No, indirect[a]	2011 Choi [32]
PETN	$PETN+NO_3^-$	1.14	SESI	No	2004 Tam Hill [13]
PETN	$PETN+NO_3^-$	1.19	ESI	No	2010 Hilton Wu [30]
PETN	$PETN+NO_2^-$	1.27	CD	No	2003 Khaymian [26]
PETN	$PETN+NO_2^-$	1.27	CD	No	2002 Tabrizchi [31]
PETN	$PETN+NO_2^-$	1.17[b]	SESI	No	2004 Tam Hill [13]

[a] 'Indirect' means that the mass and mobility measurement were not taken during the same experimental run.

[b] Although the authors did not assign this species as $PETN+NO_2^-$, the data seems to indicate this was the species detected by the IMS.

detection. The most persistent example in the literature of K_0 value discrepancies for explosives is the $TNT-H^-$ species. A literature report using ^{63}Ni-IMS and chloride ion reactant ion chemistry found the K_0 values of ten explosives and taggant chemicals [22]. The author calculated the value for the $TNT-H^-$ ion two ways. First, the author used a calibrant compound's K_0 value and then calculated the K_0 value for the unknown species using the equation:

$$K_{0,\mathrm{unk}} = K_{0,\mathrm{std}} \times \frac{t_{d,\mathrm{std}}}{t_{d,\mathrm{unk}}} \tag{3}$$

where $K_{0,\mathrm{unk}}$ is the K_0 value of the unknown compound, $K_{0,\mathrm{std}}$ is the K_0 value of the reference standard, $t_{d,\mathrm{std}}$ is the drift time (ms) of the reference standard and $t_{d,\mathrm{unk}}$ is the drift time (ms) of the unknown compound [23,24]. The second calculation method used the IMS instrumental parameters (the preferred method used by this study) and the standard reduced mobility equation:

$$K_0 = \left(\frac{L^2}{V \times t_d}\right)\left(\frac{T_0}{T}\right)\left(\frac{P}{P_0}\right) \tag{4}$$

where the squared length of the IMS drift region (L, cm) is divided by the voltage applied to pulse the ions into the IMS drift region (V, volts) multiplied by the analyte drift time (t_d, seconds) and corrected for standard temperature (T, Kelvin) and experimental pressure (P, Torr) [25].

The first calculation method found a K_0 value for the $TNT-H^-$ ion was 1.45 $cm^2\,V^{-1}\,s^{-1}$ while the second calculation method found a value of 1.59 $cm^2\,V^{-1}\,s^{-1}$. The author then chose to use the 1.45 $cm^2\,V^{-1}\,s^{-1}$ value to calculate every other species' K_0

value in the paper without providing a rationale for this choice. This 1.45 $cm^2\,V^{-1}\,s^{-1}$ value and its introduction of error into the calculation of subsequent K_0 values still persists, even when the majority of the literature reports today assign the $TNT-H^-$ ion a K_0 value of 1.54 $cm^2\,V^{-1}\,s^{-1}$ [21,33].

There are also gaps in the data for various ion sources. No literature values exist for NG ionized by a CD source (see Table 1). The peer-reviewed literature on explosives analysis with IMS also lacks reduced mobility values that have been simultaneously mass identified [21]. Simultaneous mass and mobility identification is needed to determine the exact analyte ion species detected. Inaccurate assignment of analyte ion species may lead to confusion over how to assign the correct K_0 value, especially if more than one ion species is produced during the analysis. Since SESI is the newest source of this group, no simultaneous mass-identified K_0 values for these explosives have been determined [19].

Thus, the first goal of this study was to determine if the various ion sources produced the same negative reactant ion species and if the type of reactant ion influenced the type of analyte ion(s) produced. Reactant ion formation is dependent on the drift/carrier gas, water content of the drift gas, and presence of a dopant. The ion sources must first be characterized without a dopant to enable a qualitative comparison of their reactant ions.

The second goal was to obtain accurate and reproducible K_0 values for the explosives across the ion sources; these values fill in critical gaps in the literature on IMS analyses of explosives. In order to accomplish this goal, the reduced mobility values must be simultaneously correlated with the ion species' mass identification. Few simultaneously mass-correlated K_0 values have been reported in the literature for these compounds. Some of the ion species responsible for these peaks have been mass analyzed using ion monitoring in IM-quadMS systems [8,9,28,32,34]. An accurate assignment of analyte ion species is important to avoid confusion when more than one analyte ion species is present.

2. Experimental

2.1. IM-TOFMS

The negative mode operation of the IM-TOFMS has previously been described [35]. Neutral sample vapor entered the 3 cm. IMS reaction region from the sample introduction system and was subsequently ionized by one of the ionization sources described below. The ions were then pulsed into the 18.04 cm. mobility drift region by a Bradbury–Nielsen ion shutter with a 200 μs pulse width. The ions drifted along a 503 V cm^{-1} uniform electric field against a countercurrent flow of heated nitrogen drift gas (110 °C) at a flow rate of 1 L min^{-1} and ambient pressure (approximately 700 Torr). The ions were directed through a pressure interface and ion focusing region towards the Burle multi channel plate detector (Lancaster, PA) for detection. The TOFMS extraction frequency was 25 kHz with 700 MS spectra generated every 2.5 s (the length of the TOF extraction period). Spectra were generated by software developed at Ionwerks Inc. (Houston, TX) run on the ITT Visual Information Solutions IDL Virtual Machine platform (Boulder, CO).

2.2. Chemical standards

The explosive standards TNT, NG, RDX and PETN, were purchased as solutions from Accustandard (New Haven, CT) in 1 mL glass ampoules. The TNT and RDX stock solutions were obtained at a concentration of 0.1 mg mL^{-1} in 1:1 (v:v)methanol:acetonitrile solvent. The NG stock solution was obtained at a concentration of 1.0 mg mL^{-1} in a 97:3 (v:v) ethanol:methanol solvent. PETN was obtained at a concentration of 1.0 mg mL^{-1} in methanol. HPLC grade methanol and water were purchased from Sigma Aldrich (St. Louis, MO). The nitrogen drift gas was purchased from A to L Compressed Gases, Inc. (Spokane, WA). All chemicals and gases were used without further purification.

2.3. Quantitative sample introduction

Samples were introduced into the system via a thermal desorption unit which has previously been described [36]. Briefly, an AHP Series in-line gas heater by Omegalux (Stamford, CT) was connected to 1/4 in. wide × 8 in. long aluminum tube wrapped in ultra high temperature heating tape also from Omegalux (model number STH051-040). The gas heater and heating tape were powered by two Variac variable transformers set to a 40 V output (Cleveland, OH). The moisture content (mg m^3 H_2O) of the drift gas was measured by a GE Moisture Image Series 1 moisture analyzer (Billerica, MA). The range of the measured moisture content in the drift gas was between 4.0 and 4.5 mg m^3. Samples were introduced into the desorption unit by loosely packing 5 3/4 in. flint glass disposable Pasteur pipettes from VWR International, LLC (West Chester, Pa) with untreated glass wool. Heated nitrogen gas at 90 ± 3 °C (as measured by a thermocouple attached to a handheld Fluke 73 Series III digital multimeter (Everett, WA)) passed over the sample at a flow rate of 90–110 mL gas min^{-1}. The gas flow was regulated by an Aalborg P Series rotameter (Orangeburg, New York) connected with 1/4 in. copper tubing and Swagelok fittings to the gas heater. Neutral sample vapors that evolved from the explosive standard compounds were swept into the reaction region of the ion mobility spectrometer where they were subsequently ionized by one of the ionization sources listed below.

Blank spectra were obtained before a series of sample runs to ensure the glass wool and sample holder were free of any contamination. After ensuring clean, blank spectra, 0.003 μg of NG, 2–10 μg TNT, 3–7 μg RDX, and 10–30 μg of PETN were deposited onto the glass wool using an Eppendorf 1–10 μL adjustable-volume pipette (Hauppauge, NY). The 1:1 (v:v) methanol: acetonitrile sample solvent was allowed to evaporate from the glass wool before insertion into a Pasteur pipette. The sample holder was then inserted into the aluminum tube with the pipette tip pointing into the sample inlet of the IMS. Background mass-to-charge ratio (m/z) spectra were obtained before each sample to ensure no carryover was present from the previous samples.

2.4. Ionization sources

The IM-TOFMS with accompanying ^{63}Ni ionization source has previously been described [35,37,38]. All three ion sources were placed at the open end of the IMS' ion-molecule reaction region and were open to the surrounding atmosphere. An electrospray ionization source (ESI), used to generate the reactant ions for the SESI, was constructed using a 60 μm I.D. × 145 μm O.D. fused silica capillary supplied by Polymicro Technologies, LLC (Phoeniz, AZ). The capillary was connected to a Hamilton 250 μL gas-tight sample syringe (Reno, NV) by stainless steel fittings from VICI Valco (Houston, TX). The 1:1 (v:v) methanol:water electrospray solution was sprayed at a flow rate of 3 μL min^{-1} using a KD Scientific Inc. model 210 syringe pump (Holliston, MA). A 3.5 kV negative polarity voltage bias was applied between the ESI tip and the IMS' first electrode to produce ions. The voltage bias was determined by monitoring the total ion counts and optimizing the voltage so that an average of 800–1000 counts were collected every 2.5 s TOF data extraction period. Dark counts picked up by

the MCP detector due to electronic noise ranged between 5 and 15 counts per TOF data extraction period.

The corona discharge ionization source was constructed using a 4 cm stainless steel 22 gauge needle. The end of the needle was connected to a high voltage source and a 3.5 kV negative polarity voltage bias was applied between the CDI and the first electrode in the IMS. As with the ^{63}Ni and SESI source, neutral sample vapor was ionized by reactant ions produced from the corona discharge source.

3. Results and discussion

3.1. Comparison of reactant ion species

Fig. 1 shows representative mass-to-charge ratio reactant ion spectra (20–150 Th) formed by the ^{63}Ni ionization source, the SESI source, and CD source in this system. Reactant ions are formed by the ion sources (discussed in Section 1) and then go on to form analyte ions through ion-molecule reactions [1]. The identification of reactant ions formed by a particular experimental setup is necessary to understand the analyte ions.

The reactant ions formed by the ^{63}Ni source on this instrument were HCO_2^-, NO_2^-, CO_3^-, NO_3^-, and $(HCO_2)NO_2^-$. The reactant ions formed by the SESI source were HCO_2^-, NO_2^-, CO_3^-, NO_3^-, and $(HCO_2)NO_2^-$. Two reactant ions were formed by the CD source: NO_3^- and $(HNO_3)NO_3^-$. The reactant ions, especially the HCO_2^- species, were mass identified using the TOFMS with an average mass accuracy of 260 ppm in the *m/z* range between 10 and 100 Th.

These reproducible spectra (taken over several weeks with the background spectra monitored over several months) show that ^{63}Ni and SESI sources formed the same reactant ion species but differed in the most intense reactant ions. The corona ionization source predominantly formed the NO_3^- monomer and dimer, $(HNO_3)NO_3^-$. These reactant ions concur with a report of the negative mode reactant ions formed by a CD source [9]. The literature report showed that NO_3^- monomer and dimer were the predominant reactant ions as the discharge source created increasing amounts of O_3 and NO_x neutrals. These neutrals then reacted to form NO_3^- via two pathways, followed by dimer formation [9]:

(a) $CO_3^- + NO_2 \rightarrow NO_3^- + CO_2$

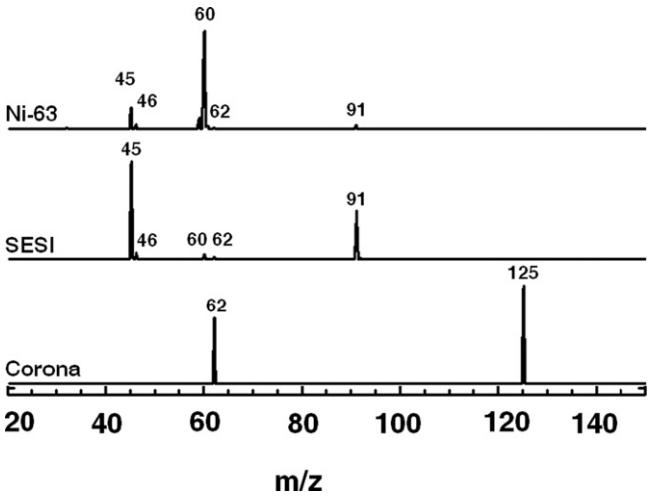

Fig. 1. Mass spectra (20–150 Th) of the reactant ions formed by the ^{63}Ni, secondary electrospray, and corona discharge ionization sources. The peak intensities are all on the same scale with the scale normalized to the highest intensity peak.

(b) $NO_2^- + O_3 \rightarrow NO_3^- + O_2$

(c) $NO_3^- + HNO_3 \rightarrow (HNO_3)NO_3^-$ (5)

For this experimental setup, no additional reactant ion chemistry (i.e., dopant chemistry) was used so that a baseline reactant ion species profile could be established for each of the sources used in this study. Commercial ion mobility spectrometers use a combination of reactant ion chemistry (typically chloride vapor) and gas dehumidification and purification to ensure reproducible reactant ion species [1]. However, even small gas impurities (i.e., >1 ppm CO_2) and changes in humidity level can influence the reactant ion species profile; [9] this change in ion species profile may, in turn, cause different or unexpected analyte ions to form for a particular analyte.

Purified nitrogen was used as the drift gas instead of air to ensure uniform drift gas composition and accurate K_0 value determinations. With a ^{63}Ni source, the typical reactant ions in pure N_2 are electrons and in air are O_2^-, $(H_2O)O_2^-$, and $(CO_2)O_2^-$ [1]. However, the ion sources were operated in air due to instrumental constraints and small amounts of air were present in the IMS due to back-diffusion of room air into the system. Attempts were made to mitigate this problem by a 1 L min^{-1} flow rate of nitrogen to flush the system of air but the experimental setup still allowed in small amount of air next to the ion source. The setup discussed here is similar to a study comparing negative reactant ions produced in air, N_2, and SF_6 using IM-quadMS [5]. The presence of *m/z* 45, assigned as HCO_2^-, and *m/z* 91, $(HCO_2)NO_2^-$, were persistently found in both the air and N_2 reactant ion spectra. These species may have been present in the room air, in the gas cylinders, or from another source in the experimental setup but were consistently seen in reactant ion spectra over the course of this study. Select K_0 values for reactant and analyte ions found in this study were also benchmarked against K_0 values found in air on this same system as tracked over several years. Percent differences for the K_0 values found in air versus nitrogen varied between 0.2 and 3.0% (see Supplementary information).

4. Accurate determination of mass-identified mobility values for explosives with various ion sources

Table 2 summarizes the analyte ion identifications and average reduced mobility values for each explosive analyzed by each ion source. The ion identifications and K_0 value determinations are discussed in the sections below.

Table 2
Reduced mobility values of explosives for simultaneously mass-identified mobility peaks. The ID of the mass peak along with the average K_0 value found in this study is given to one standard deviation for sample sizes (n) of 3–5.

Explosive	Ionization source	Major analyte ion *m/z* (Th)	Ion identification	Avg. K_0 value ($cm^2\,V^{-1}\,s^{-1}$)
TNT	Nickel-63	226	$TNT-H^-$	1.540 ± 0.004
	SESI	226	$TNT-H^-$	1.530 ± 0.004
	Corona	226	$TNT-H^-$	1.540 ± 0.009
NG	Nickel-63	289	$NG+NO_3^-$	1.350 ± 0.007
	SESI	289	$NG+NO_3^-$	1.350 ± 0.020
	Corona	289	$NG+NO_3^-$	1.330 ± 0.010
PETN	Nickel-63	378	$PETN+NO_3^-$	1.160 ± 0.008
	SESI	378	$PETN+NO_3^-$	1.160 ± 0.008
	Corona	378	$PETN+NO_3^-$	1.160 ± 0.006
RDX	Nickel-63	268	$RDX+NO_2^-$	1.390 ± 0.030
	SESI	268	$RDX+NO_2^-$	1.420 ± 0.002
	Corona	284	$RDX+NO_3^-$	1.380 ± 0.006

4.1. ^{63}Nickel ionization

Fig. 2 shows representative mass-to-charge ratio spectra (from 200 to 400 Th) and simultaneously collected mobility drift time spectra (15.0–22.0 ms) for four explosives ionized by the conventional ^{63}Ni ion source. The analyte ion spectra of TNT shows a proton abstracted TNT$-$H$^-$ species at 226 Th with a corresponding mobility peak at 1.540 ± 0.004 cm^2 V^{-1} s^{-1} (where the sample size (n)=4). This value agrees with literature reports for the reduced mobility value of TNT at 1.54 cm^2 V^{-1} s^{-1}. [21] This value also provides further evidence that the true mobility value of TNT's proton abstracted ion is 1.54 cm^2 V^{-1} s^{-1} and not the widely reported value of 1.45 cm^2 V^{-1} s^{-1} when measured at temperatures above 150 °C [24, 23].

The analyte ion spectra for RDX shows a RDX+NO_2^- adduct species at 268 Th and a corresponding mobility value of 1.39 ± 0.030 (n=4). This value is slightly lower than the most commonly reported value of 1.43 cm^2 V^{-1} s^{-1} [21]. However, the experimental and literature value may both be inaccurate due to several reasons. First, the K_0 value may be inaccurate due to suspected thermal instability of RDX. As seen in Fig. 2, the width of the RDX mobility peak is narrower than the other mobility peaks. This narrow peak is an anomaly due to inefficient sample vaporization because RDX has the lowest vapor pressure out of all the explosives surveyed and has notorious thermal degradation issues [21]. However, while the spectral data shows a narrow peak due to low ion count statistics, the ion counts are above the signal:noise ratio threshold (15 counts) required to obtain K_0 information. Furthermore, the K_0 data was reproducible even though the RDX peaks for the ^{63}Ni work had lower S:N ratios than the other explosives. The rest of the peaks in the entire study all share similar mobility peak widths. These peak widths, measured with resolving powers between 70 and 100, were representative of individual ion peaks and not overlapping ion species. This value is also not statistically different from the K_0 value obtained for the same ion species using the SESI source at $\pm 1\sigma$.

Second, the methods used to vaporize and ionize RDX in the literature were found using laser desorption before ^{63}Ni ionization whereas this work used direct thermal desorption before ionization [39]. Finally, the literature mobility value of the RDX+Cl^- species was reported as 1.40 cm^2 V^{-1} s^{-1} and the other most common species, RDX+NO_3^-, was reported at 1.39 cm^2 V^{-1} s^{-1}. Since these two values are only slightly different, low resolving power IMS systems (where the measured resolving power is defined as the ability to separate peaks in IMS and is calculated using the mobility drift time of the ion species divided by the peak width at half-height) may not have been able to distinguish between the two ion species of RDX and, therefore, may not have been able to detect subtle shifts in the IMS ion chemistry.

The analyte ion spectra for NG shows a NG+NO_3^- species at 289 Th and a mobility peak with a value of 1.35 ± 0.007 cm^2 V^{-1} s^{-1} (n=4). The mobility literature values for this species ranged from 1.32, 1.37, or 1.40 cm^2 V^{-1} s^{-1} [21]. A range of K_0 values in the literature may indicate that this K_0 value is temperature-dependent [23]. Several reports have shown that K_0 values can vary with temperature and that certain compounds were more sensitive to temperature fluctuations than others [23,40,41]. An average literature value of 1.36 cm^2 V^{-1} s^{-1} matched more closely with the value found in this study [21].

The analyte ion spectra for PETN shows three ions: a PETN$-$H$^-$ species at 315 Th and 1.25 ± 0.007 cm^2 V^{-1} s^{-1} (n=3); PETN+NO_2^- ion at 362 Th with a mobility value of 1.190 ± 0.009 cm^2 V^{-1} s^{-1} (n=4); and a PETN+NO_3^- ion at 378 Th and 1.160 ± 0.008 cm^2 V^{-1} s^{-1} (n=4). There is no reported literature value for the PETN+NO_2^- species and the literature value for the PETN+NO_3^- species is 1.10 cm^2 V^{-1} s^{-1} although the literature study did not mass-identify the species at 1.10 cm^2 V^{-1} s^{-1} [21]. The discrepancy between the literature and experimental values for the PETN+NO_3^- species may be due to inaccurate assignment of ion species by inference on standalone IMS systems (i.e., confusing the PETN+NO_3^- for the PETN+Cl^- species which has a literature value of 1.15 cm^2 V^{-1} s^{-1}) [42]. The historically low resolving power of IMS systems in previous reports ($Rp < 40$) may have also obscured the detection of ion species with similar K_0 values, which may have only produced a somewhat more broad peak than the reactant ion peak (RIP) in the mobility spectra [43,44].

4.2. Secondary electrospray ionization

Fig. 3 shows representative mass-to-charge ratio spectra (from 200 to 400 Th) and simultaneously collected mobility drift time spectra (15.0–22.0 ms) for four explosives ionized by a secondary electrospray ionization (SESI) source. The analyte ion spectra of TNT shows a proton abstracted TNT$-$H$^-$ species at 226 Th with a mobility peak at 1.530 ± 0.004 cm^2 V^{-1} s^{-1} (n=4). This value agreed with literature reports for the reduced mobility value of

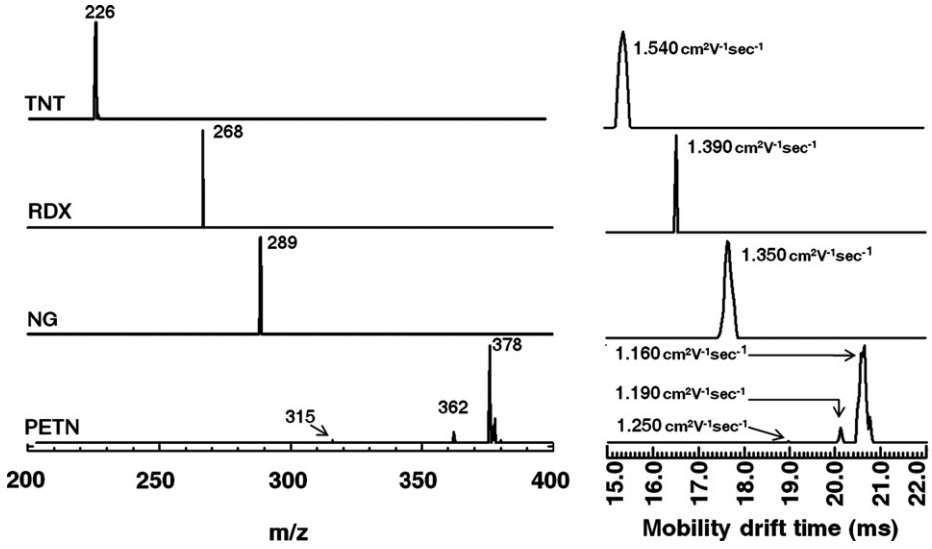

Fig. 2. Mass-to-charge ratio spectra (200–400 Th) and mobility drift time spectra (15.0–22.0 ms) of TNT, RDX, NG, and PETN explosives ionized by ^{63}Ni.

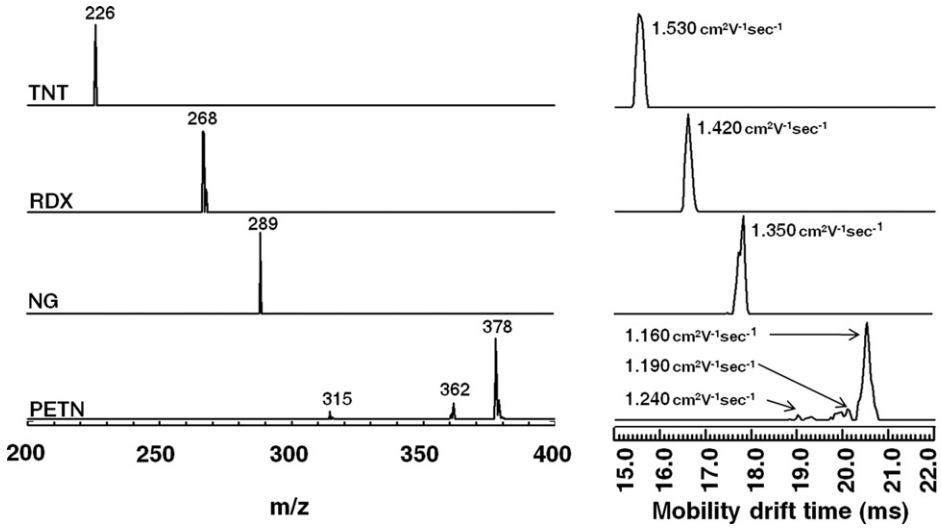

Fig. 3. Mass-to-charge ratio spectra (200–400 Th) and mobility drift time spectra (15.0–22.0 ms) of TNT, RDX, NG, and PETN explosives ionized by secondary electrospray ionization.

TNT at 1.54 $cm^2\,V^{-1}\,s^{-1}$ found with a SESI source [19]. This value also agreed with the K_0 value found for TNT$-H^-$ with the ^{63}Ni source in this study.

The analyte ion spectra for RDX shows a RDX$+NO_2^-$ adduct species at 268 Th and a corresponding mobility value of 1.42 ± 0.002 $cm^2\,V^{-1}\,s^{-1}$. This value matches closely with the most commonly reported value of 1.43 $cm^2\,V^{-1}\,s^{-1}$ for the ion species collected with a ^{63}Ni source and for the value reported with the SESI source at 1.40 $cm^2\,V^{-1}\,s^{-1}$ [19,21]. Again, the discrepancies with this mobility value in the literature point to changes in the analyte ion chemistry and thermal instability of RDX. More accurate and reproducible work beyond this study is needed to fully characterize the mobility values for each RDX ion.

The analyte ion spectra for NG show a NG$+NO_3^-$ species at 289 Th and a mobility peak corresponding to a value of 1.35 ± 0.020 $cm^2\,V^{-1}\,s^{-1}$ ($n=3$). There was only one literature report for the K_0 value of NG with SESI at 1.31 $cm^2\,V^{-1}\,s^{-1}$ [19]. The experimental value found here matched more closely with an average literature value of 1.36 $cm^2\,V^{-1}\,s^{-1}$ found using the ^{63}Ni source and the literatures values for NG with ^{63}Ni sources.

The analyte ion spectra for PETN shows three mass-identified mobility peaks: a proton abstracted PETN$-H^-$ species at 315 Th and 1.24 ± 0.008 $cm^2\,V^{-1}\,s^{-1}$ ($n=3$); a PETN$+NO_2^-$ adduct at 362 Th and 1.190 ± 0.004 $cm^2\,V^{-1}\,s^{-1}$($n=3$); and a PETN$+NO^-$ adduct species at 378 Th and 1.160 ± 0.008 $cm^2\,V^{-1}\,s^{-1}$ ($n=3$). The experimental value for the PETN$-H^-$ species agrees well with the SESI literature value at 1.25 $cm^2\,V^{-1}\,s^{-1}$; the ^{63}Ni value for this species is 1.22 $cm^2\,V^{-1}\,s^{-1}$ although this value was calculated using a K_0 value of TNT at 1.45 $cm^2\,V^{-1}\,s^{-1}$ instead of 1.54 $cm^2\,V^{-1}\,s^{-1}$ [19,42]. There is no reported literature value for the PETN$+NO_2^-$ species either by SESI or ^{63}Ni although the previous SESI-IMS study found an unidentified ion for PETN with a K_0 of 1.17 $cm^2\,V^{-1}\,s^{-1}$ that is most likely the PETN$+NO_2^-$ adduct. The literature value for the PETN$+NO_3^-$ species with a SESI source is 1.14 $cm^2\,V^{-1}\,s^{-1}$ which agrees closely with the 1.160 ± 0.008 $cm^2\,V^{-1}\,s^{-1}$ ($n=5$) value found in this study. The ^{63}Ni literature value for this species is 1.10 $cm^2\,V^{-1}\,s^{-1}$ although, again, this value was calculated using a K_0 value of TNT at 1.45 $cm^2\,V^{-1}\,s^{-1}$ instead of 1.54 $cm^2\,V^{-1}\,s^{-1}$ [19,42].

PETN has recently become a greater explosive of interest since it was used in the attempted 2009 Christmas Day bombing on Northwest flight 253 from Amsterdam to Detroit, Michigan [45]. PETN has also been readily available as an explosive of opportunity since it can be removed from detonation cord to create improvised explosive devices [46]. These three analyte ions may serve as a 'fingerprint' for PETN in the mobility-mass spectra and greatly increase the chance of detecting PETN in a sample with a complex matrix. The confirmation of these PETN 'fingerprint' ions may then decrease the false positive rates for commercial IMS systems deployed in the field.

4.3. Corona discharge ionization

Fig. 4 shows representative mass-to-charge ratio spectra (from 200 to 400 Th) and simultaneously collected mobility drift time spectra (15.0–22.0 ms) for four explosives ionized by a corona discharge (CD) ionization source. The mobility and mass spectra of TNT collected with a CD source shows a proton abstracted TNT$-H^-$ species at 1.54 $cm^2\,V^{-1}\,s^{-1}$ ± 0.009 ($n=4$) and 226 Th. This species was seen with each ion source studied and reflects the most common negative ionization formation route for TNT in the presence of O_2. An acidic proton on the methyl group of the 2,4,6-trinitrotoluene molecule was abstracted by an electronegative reactant ion species produced by the CDI (i.e., where $X=O_2^-, CO_3^-$) via the reaction:

$$\text{TNT} + X^- \rightarrow \text{TNT-}H^- + HX \quad (6)$$

The ion source may produce varying electronegative reactant ions but the resultant ion species for TNT remains the same, regardless of the sources surveyed in this study.

The mobility and mass spectra for RDX shows a change in analyte ion chemistry with the CD source versus the ^{63}Ni and SESI sources. With the changed reactant ion species profile, the primary RDX analyte ion species shifted from RDX$+NO_2^-$ at 268 Th and 1.43 $cm^2\,V^{-1}\,s^{-1}$ to RDX$+NO_3^-$ at 284 Th and 1.38 $cm^2\,V^{-1}\,s^{-1}$ ± 0.006 ($n=4$). In the presence of the ^{63}Ni and SESI sources, RDX auto-ionized to form the RDX$+NO_2^-$ species; in the presence of the CD source, the overwhelming concentration of NO_3^- ions from the CD source caused the RDX to adduct with the NO_3^- reactant ion instead of auto-ionizing to form the primary analyte ion. When the K_0 values are compared for the two RDX adduct species produced with the CD and ESI sources, the nitrite adduct has a higher mobility value than the nitrate adduct. This trend is also reported in the literature for these same species (see Table 1).

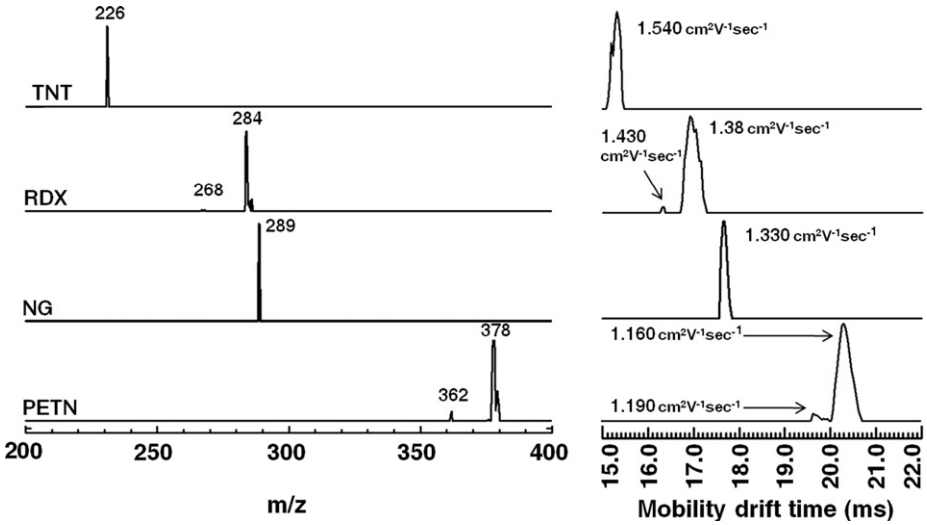

Fig. 4. Mass-to-charge ratio spectra (200–400 Th) and mobility drift time spectra (15.0–22.0 ms) of TNT, RDX, NG, and PETN explosives ionized by corona discharge ionization.

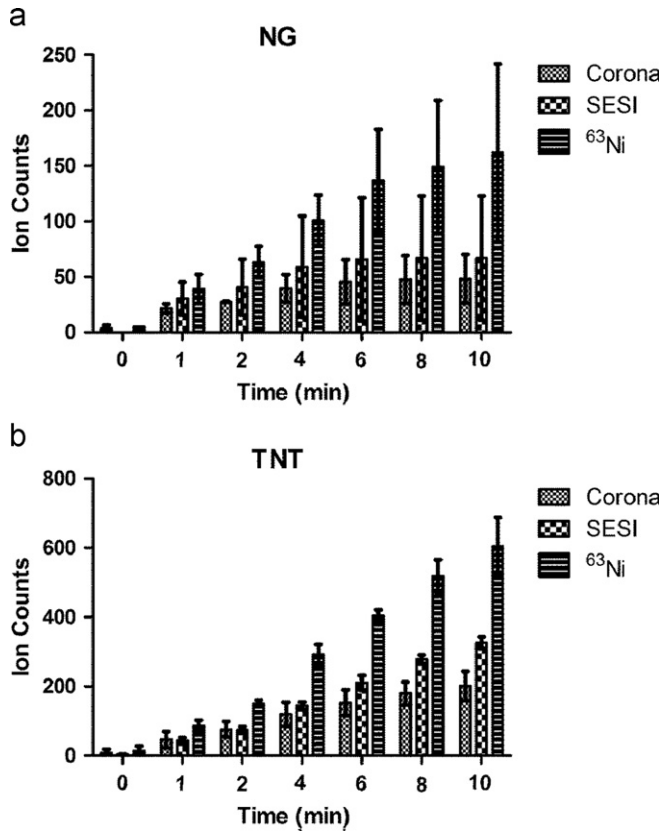

Fig. 5. Ion counts vs. time (minutes) for (a) NG and (b) TNT when ionized by three ion sources: corona discharge, SESI, and ^{63}Ni. The MS ion counts were monitored for the ion species NG$+NO_3^-$ at *m/z* 289 and the TNT$-H^-$ ion at *m/z* 226 with a $\pm$0.5 Da window on either side from the center of the peak.

The mobility and mass spectra for NG shows a NG$+NO_3^-$ species at 289 cm^2 V^{-1} s^{-1}Th and a mobility peak corresponding to a value of 1.33 ± 0.010 cm^2 V^{-1} s^{-1} (n=4). There were no literature reports for the mobility value of NG with a CD source. The experimental value found here matched closely with an average literature value of 1.36 cm^2 V^{-1} s^{-1} found using ^{63}Ni sources and the SESI value at 1.31 cm^2 V^{-1} s^{-1} [19,21].

The mobility and mass spectra for PETN showed a PETN$+NO_3^-$ adduct at 362 Th and 1.190 ± 0.004 cm^2 V^{-1} s^{-1} (n=4) and a PETN$+NO_3^-$ adduct species at 378 Th and 1.160 ± 0.006 cm^2 V^{-1} s^{-1} (n=4). A literature value has not been reported for the PETN$+NO_2^-$ species by any of the sources surveyed in this study; there was no reported literature value for the PETN$+NO_3^-$ species for a CD source. The ^{63}Ni K_0 value for this species was 1.10 cm^2 V^{-1} s^{-1}; however, this value was calculated using a K_0 value of TNT at 1.45 cm^2 V^{-1} s^{-1} instead of 1.54 cm^2 V^{-1} s^{-1} [19,42]. The PETN$-H^-$ species was not present with the CD source presumably due to the reactant ion chemistry. The PETN$+NO_2^-$ and PETN$+NO_3^-$ species were most likely favored to form due to the formation of NO_3^- reactant ions which caused adduct formation over proton abstraction reactions.

5. Quantitative comparison of the IMMS response for explosives ionized by ^{63}Ni, SESI, and corona ionization sources

Fig. 5 shows a plot of MS ion counts vs. time for (a) NG and (b) TNT collected in the IMMS data acquisition mode using each ion source: CD, SESI, and ^{63}Ni. The MS ion counts were monitored for the ion species NG$+NO_2^-$ at *m/z* 289 and the TNT$-H^-$ ion at *m/z* 226 with a $\pm$0.5 Da window on either side from the center of the peak. The ion counts were tracked over a ten minute period and recorded at two minute intervals. The start of IMMS data acquisition and the start of sample introduction were synchronized and began at time=0 min. 0.003 μg of NG and 10.0 μg of TNT were introduced via thermal desorption into the ion-molecule reaction region of the IMS. The plots show that, for both NG and TNT, the ^{63}Ni source had the highest ion counts over the acquisition period, followed by SESI, and then the CD source. $\pm 1\sigma$ error bars are given for a sample size (n) of three.

6. Conclusion

This study found the reactant ion and analyte ion species for three ion sources analyzing conventional explosives: conventional ^{63}Ni, secondary electrospray ionization, and corona discharge ionization. The study also established accurate and reproducible mass-identified reduced mobility values for the explosives with each ion source. The conventional ^{63}Ni source has a proven track record of ionization for the above listed compounds; however, the SESI source produced the same ion species as the ^{63}Ni source except for PETN where it produced a third ion species, PETN$-H^-$. This third ion species was beneficial

for PETN detection because it provided a third way to identify PETN if the compound were part of a complex matrix.

The CD source also compared well with ^{63}Ni but produced a different primary analyte ion for RDX. This change in primary analyte ion species was influenced by the reactant ion species profile of the CD. The reactant ion species profile for CD was distinctly different from either the ^{63}Ni or SESI source. Careful work with CD should be performed to detect other analyte ion changes for other explosives. Overall, the SESI source most closely reproduced the reactant ion species and analyte ion species profiles for ^{63}Ni. This source is a non-radioactive, robust, and flexible alternative for ^{63}Ni. CD, with its different reactant ion chemistry, may be less effective as a replacement for radioactive ^{63}Ni sources.

Acknowledgements

This project was funded in part by Grant no. 0731306 from the U.S. National Science Foundation.

Appendix A. Supporting information

Supplementary data associated with this article can be found in the online version at http://dx.doi.org/10.1016/j.talanta.2013.01.009.

References

[1] G. Eiceman, Z. Karpas, Ion Mobility Spectrometry, CRC Press, 2005.
[2] G. Spangler, et al., J. Test. Eval. 13 (1985) 234–240.
[3] K.A. Daum, et al., Talanta 55 (2001) 491–500.
[4] K.A. Daum, et al., Int. J. Mass Spectrom. 214 (2001) 257–267.
[5] T.W. Carr, Anal. Chem. 51 (1979) 705–711.
[6] S.K. Ross, A.J. Bell, Int. J. Mass Spectrom. 218 (2002) L1–L6.
[7] Smiths, and Detection (2008). Smiths Detection Wins $65 Million Contract for JCAD Chemical Detectors. Volume, DOI:.
[8] C.A. Hill, C.L.P. Thomas, Analyst 128 (2003) 55–60.
[9] R.G. Ewing, M.J. Waltman, Int. J. Ion Mobility Spectrom. (2009) 65–72.
[10] M.J. Waltman, et al., Talanta 77 (2008) 249–255.
[11] Y.H. Chen, et al., J. Microcolumn Sep. 6 (1994) 515–520.
[12] W.E. Steiner, et al., Anal. Chem. 75 (2003) 6068–6076.
[13] M. Tam, H.H. Hill, Anal. Chem. 76 (2004) 2741–2747.
[14] C. Wu, et al., Anal. Chem. 72 (2000) 396–403.
[15] J. Fernandez de la Mora, Int. J. Mass Spectrom. 300 (2011) 182–193.
[16] P. Martínez-Lozano, et al., J. Am. Soc. Mass. Spectrom. 20 (2009) 287–294.
[17] L.A. Dillon, et al., Analyst 135 (2010) 306–314.
[18] C.-Y. Lee, J. Shiea, Anal. Chem. 70 (1998) 2757–2761.
[19] M. Tam, H. Herbert, J. Hill, Anal. Chem. 76 (2004) 2741–2747.
[20] Whitehouse, C.M., et al. (1986), in: 34th ASMS Conference on Mass Spectrometry and Allied Topics, p. 507.
[21] R.G. Ewing, et al., Talanta 54 (2001) 515–529.
[22] Danylewych-May, L.L., Cumming, C. (1993) Explosive and taggant detection with ionscan, in: Advances in Analysis and Detection of Explosives, Yinon, J., (Ed.), 385-401.
[23] G.A. Eiceman, et al., Anal. Chim. Acta 493 (2003) 185–194.
[24] Danylewych-May, L.L. (1990) Modifications to the Ionization Process to Enhance the Detection of Explosives by IMS. 672-686, Barringer Research Limited.
[25] E.A. Mason, E.W. McDaniel, Transport Properties of Ions in Gases, Wiley, 1988.
[26] T. Khaymian, et al., Talanta 59 (2003) 327–333.
[27] K.M. Roscioli, et al., Anal. Chem. 83 (2011) 5965–5971.
[28] J. Laakia, et al., Rapid Commun. Mass Spectrom. 23 (2009) 3069–3076.
[29] F.A. Fernandez-Lima, et al., Russ. J. Phys. Chem. A 113 (2009) 8221–8234.
[30] C.K. Hilton, et al., Int. J. Mass Spectrom. 298 (2010) 64–71.
[31] M. Tabrizchi, A. Abedi, Int. J. Mass Spectrom. 218 (2002) 75–85.
[32] S.-S. Choi, et al., Bull. Korean Chem. Soc. 32 (2011) 1055–1058.
[33] G.W. Cook, et al., Indian J. Forensic Sci. 55 (2010) 1582–1591.
[34] M. Sabo, et al., Int. J. Mass Spectrom. 293 (2010) 23–27.
[35] W.E. Steiner, et al., Rapid Commun. Mass Spectrom. 15 (2001) 2221–2226.
[36] C.L. Crawford, et al., Anal. Chem. 82 (2010) 387–393.
[37] W.E. Steiner, et al., Anal. Chem. 74 (2002) 4343–4352.
[38] W.E. Steiner, et al., Anal. Chem. 77 (2005) 4792–4799.
[39] S.D. Huang, et al., Appl. Spectrosc. 41 (1987) 1371–1376.
[40] R. Fernández-Maestre, et al., Anal. Chem. (2009).
[41] G. Kaur-Atwal, et al., Int. J. Ion Mobility Spectrom. 12 (2009) 1–14.
[42] Danylewych-May, L.L. (1991) Modifications to the ionization process to enhance the detection of explosivs by IMS, in: Proceedings of the First International Symposium on Explosive Detection Technology, pp. 672–686.
[43] W.F. Siems, et al., Anal. Chem. 66 (1994) 4195–4201.
[44] A.B. Kanu, et al., Anal. Chem. 80 (2008) 6610–6619.
[45] Hsu, S.S. (2009) Airplane bomb plot on Christmas Day exposes air security weaknesses, in: The Washington Post.
[46] P.W. Cooper, S.R. Kurkowski, Introduction to the Technology of Explosives, Wiley-VCH, 1996.